Molecular dissection of hippocampal theta-burst pairing potentiation

D. A. Hoffman*, R. Sprengel, and B. Sakmann

Abteilung Zellphysiologie and Molekulare Neurobiologie, Max-Planck Institut für medizinische Forschung, Jahnstrasse 29, D-69120 Heidelberg, Germany

Contributed by B. Sakmann, March 18, 2002

Long-term potentiation (LTP) of synaptic efficacy in the hippocampus is frequently induced by tetanic stimulation of presynaptic afferents or by pairing low frequency stimulation with postsynaptic depolarization. Adult (P42) GluR-A$^{-/-}$ mice largely lack these forms of LTP. LTP in wt mice can also be induced by coincident pre- and postsynaptic action potentials, where an initial rapid component is expressed but a substantial fraction of the potentiation develops with a delayed time course. We report here that this stimulation protocol, delivered at theta frequency (5 Hz), induces LTP in GluR-A$^{-/-}$ mice in which the initial component is substantially reduced. The remaining GluR-A independent component differs from the initial component in that its expression develops over time after induction and its induction is differentially dependent on postsynaptic intracellular Ca^{2+} buffering. Thus, in adult mice, theta-burst pairing evokes two forms of synaptic potentiation that are induced simultaneously but whose expression levels vary inversely with time. The two components of synaptic potentiation could be relevant for different forms of information storage that are dependent on hippocampal synaptic transmission such as spatial reference and working memory.

Long-term changes in synaptic efficacy in the hippocampus can be induced by different patterns of stimulation generating pre- and postsynaptic depolarization: e.g., by high frequency stimulation applied to the presynaptic cell (1) or by low frequency presynaptic stimulation paired with prolonged postsynaptic depolarization (2–4). By using these protocols, the peak increase in synaptic efficacy is expressed rapidly (1–3 min) after the stimulation epoch. On the other hand, theta-burst pairing (TBP), a coincident pre- and postsynaptic stimulation, generates a rapid potentiation of synaptic strength that then increases with time (5, 6). The difference in the time course of expression of long-term potentiation (LTP) suggests different expression mechanisms for the rapid and slow components.

GluR-A-deficient mice (GluR-A$^{-/-}$) do not express LTP induced by 100 Hz tetanus, and LTP is strongly reduced with depolarization pairing protocols (7, 8). We show here, however, that TBP in GluR-A$^{-/-}$ mice induces a slow developing, delayed potentiation (delTBP potentiation) that becomes indistinguishable from that found in wt mice 25 min postinduction. The size of this slow developing component of TBP potentiation was correlated with complex spiking induced during the pairing (6, 9). The potentiation induced initially after TBP (iniTBP potentiation) in wt mice is, however, greatly reduced in adult GluR-A$^{-/-}$ mice. This GluR-A-dependent component of TBP potentiation is transient and more sensitive to intracellular Ca^{2+} buffers than delTBP potentiation. Thus, in adult mice, TBP evokes two forms of potentiation.

Methods

Adult (P41-56) wt (C57BL6) and GluR-A$^{-/-}$ (7) mice were deeply anesthetized with halothane. After removal of the brain in ice-cold modified ACSF cutting solution (in mM, 125 NaCl/2.5 KCl/1 $MgCl_2$/2 $CaCl_2$/25 glucose/1.25 NaH_2PO_4/0.4 ascorbic acid/3 *myo*-inositol/2 sodium pyruvate/25 $NaHCO_3$), 250-μm-thick, transverse hippocampal slices were prepared. The slices were incubated, submerged in a holding chamber for 10 min at 34°C, and then stored at room temperature in ACSF solution containing the cutting solution. For whole-cell recordings, slices were transferred to a submerged recording chamber with continuous flow of ACSF containing (in mM) 125 NaCl, 25 $NaHCO_3$, 2.5 KCl, 1.25 NaH_2PO_4, 2 $CaCl_2$, 1 $MgCl_2$, and 25 glucose, along with 10 μM bicuculline. 2-amino-5-phosphonovaleric acid (APV; 50 μM) and 20 μM MK-801 (Tocris Neuramin, Bristol, U.K.) were added to the ACSF in some experiments. All cutting and recording external solutions were bubbled with 5% CO_2/95% O_2.

Hippocampal neurons were identified by using infrared differential interference contrast videomicroscopy. The patch electrodes (2–7 MΩ) were filled with (in mM): 125 potassium gluconate/20 KCl/10 Hepes/10 phosphocreatine/4 ATP-Mg/0.3 GTP/0–10 EGTA or 1,2-bis(2-aminophenoxy)ethane-*N*,*N*,*N*′,*N*′-tetraacetic acid (BAPTA; pH 7.2 with KOH). The normal internal solution contained no calcium buffers, but in some cases these results were pooled with those including 0.5 mM EGTA as the groups showed similar potentiation. Whole-cell recordings were made in current-clamp mode by using an Axopatch-200B (Axon Instruments, Foster City, CA). Only data from cells with resting membrane potentials larger than −60 mV were analyzed. To evoke synaptic potentials, glass electrodes filled with ACSF were placed within 50 μm lateral to the dendrite in stratum radiatum and stratum oriens. Stimuli (100 μs) were evoked at 0.2 Hz at an intensity adjusted to produce a single excitatory postsynaptic potential (EPSP) with an average amplitude of 1 to 5 mV at the beginning of recordings. At the beginning and end of each experiment, pathway independence was tested by using a cross-paired pulse facilitation protocol. EPSPs in the paired and control pathways were stimulated 1 s apart. Series and input resistances were continuously monitored during the recording in response to a small, 100-ms, hyperpolarizing pulse at the beginning of evoked EPSPs. The series resistance (read from the amplifier dial) ranged from 10 to 40 MΩ. If the electrode clogged during the experiment, it was either cleared by applying positive pressure or the seal was lost in the attempt. All recordings were made at 32–34°C.

The pairing protocol consisted of coincident EPSPs and postsynaptic action potential (APs; 1–2 nA postsynaptic current injection for 2 ms) paired five times at 100 Hz. Five paired bursts were given at 5 Hz to constitute a theta train. Three trains (0.1 Hz) were given in total. Under our experimental conditions the 100-Hz burst of EPSPs, when given without paired APs, was often suprathreshold. Thus, in the unpaired controls, the postsynaptic cell was voltage clamped to −70 mV. The amplitude of a synaptic response was calculated as the difference between the peak average of 5 data points, acquired at 5 kHz, in a 250-point window around the peak of the synaptic response and a 100-point average immediately preceding the stimulus. The

Abbreviations: LTP, long term potentiation; AP, action potential; TBP, theta burst pairing; delTBP, delayed TBP; iniTBP, initial TBP; EPSP, excitatory postsynaptic potential; wt, wild type; NMDA, *N*-methyl-D-aspartate; BAPTA, 1,2-bis(2-aminophenoxy)ethane-*N*,*N*,*N*′,*N*′-tetraacetic acid.

*To whom reprint requests should be addressed. E-mail: dax@sun0.MPImF-Heidelberg.mpg.de.

www.pnas.org/cgi/doi/10.1073/pnas.092157999

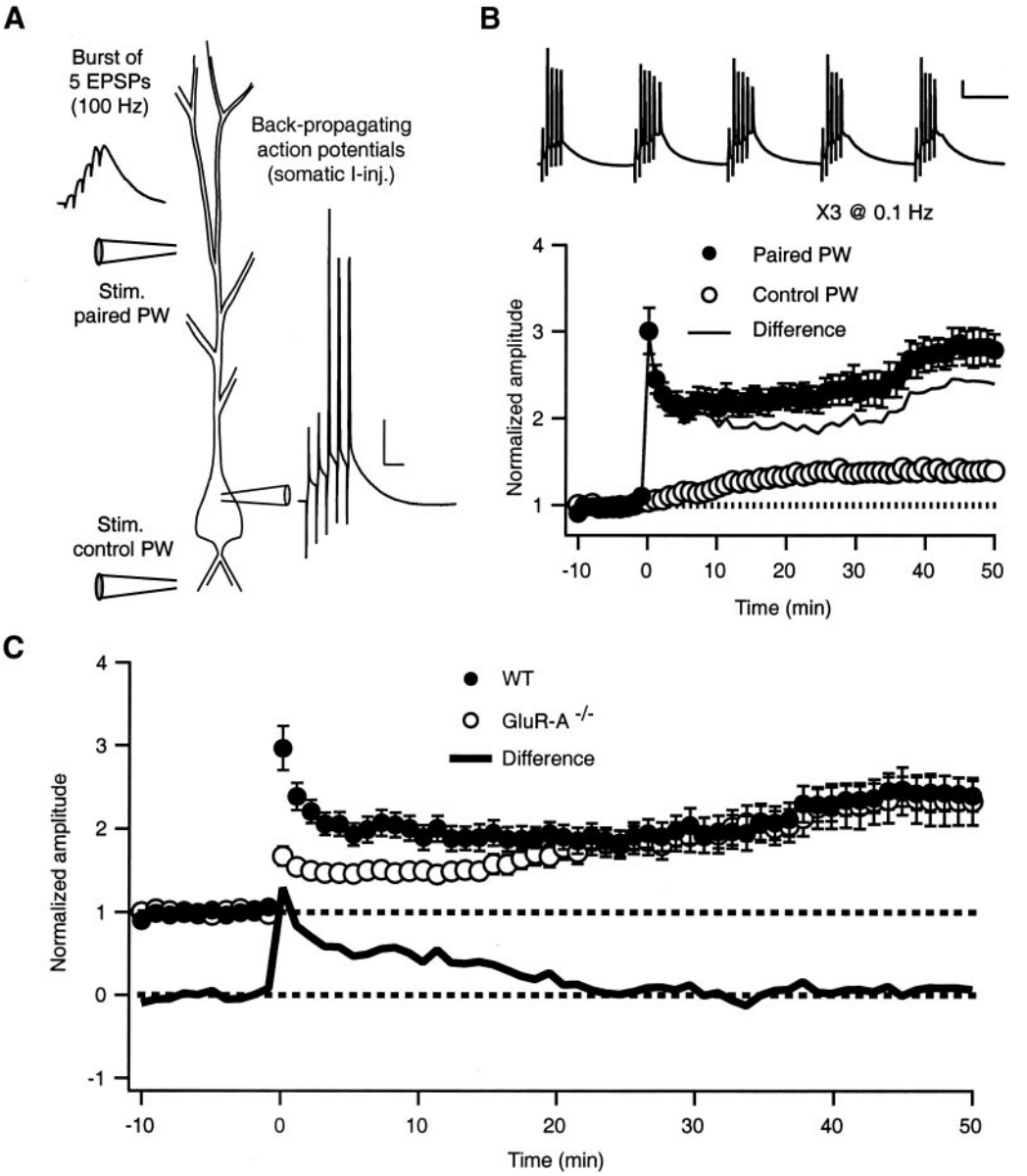

Fig. 1. Theta-burst pairing induces LTP in hippocampal CA3-CA1 synapses of wt and GluR-A$^{-/-}$ mice. (*A*) The TBP protocol consisted of coincident EPSPs delivered via a glass field stimulating electrode (*Left* trace) and postsynaptic APs (1–2 nA, 2 ms somatic current injection, *Right* trace) paired five times at 100 Hz. A second stimulating electrode was used for a control pathway and thus not stimulated during the TBP protocol. Scale bar = 20 mV, 20 ms (*B*) Five paired bursts were given at 5 Hz to constitute the train shown (*Top* trace; note complex spiking in the second and third paired bursts). Scale bar = 20 mV, 100 ms. Three trains (0.1 Hz) of paired stimulation resulted in a potentiation with a complex time course in the paired pathway in wt mice (filled circles). A small but significant potentiation in the control pathway (open circles) was also consistently observed. Subtraction of the two pathways gives the solid line. (*C*) TBP in slices from GluR-A$^{-/-}$ mice (open circles) resulted in a long-lasting, robust potentiation of synaptic inputs, which was identical to wt (filled circles) about 25 min postpairing. GluR-A$^{-/-}$ mice, however, lack the large, rapidly expressed component of TBP potentiation found in WT mice. Subtracting the GluR-A$^{-/-}$ curve from the wt curve gives the difference component shown below (solid line). The GluR-A subunit-sensitive component is induced immediately after pairing but is transient, reaching baseline about 25 min postinduction.

average response of the final 5–15 min immediately before LTP induction (of 5–20 min total) was taken as the baseline, and all values were normalized to this number. Cells not showing a stable baseline within 20 min of break-in were discarded. In summary plots, the reported EPSPs are 1-minute averages. Values are expressed as means ± SE. Two-tailed *t* tests were used for calculation of the statistical significance of differences.

Results

Fig. 1*A* illustrates the theta-burst pairing protocol used to induce a long-lasting potentiation of EPSP amplitudes in wt and GluR-A$^{-/-}$ mice. Short, presynaptic bursts of Schaffer-collateral stimulation were paired one-to-one with postsynaptic current injections to initiate back-propagating action potentials. These paired bursts were repeated five times at 5 Hz to constitute the train shown in Fig. 1*B Upper*. Fig. 1*B Lower* shows the potentiation resulting from TBP in wt. In the paired pathway, after an initial peak, the EPSP amplitude decays over the first few minutes postinduction before slowly increasing with time until it levels out about 45 min postpairing. A control pathway monitored EPSP amplitude in an independent set of synapses before and after TBP (Fig. 1 *A* and *B*). We also found a small increase in

Table 1. TBP potentiation as percentage of control

Treatment	Time, min	wt % pot.	wt *n*	wt *t* test	GluR-A$^{-/-}$ % pot.	GluR-A$^{-/-}$ *n*	GluR-A$^{-/-}$ *t* test
EGTA							
(0–0.5)	5	100 ± 6	29	—	44 ± 5	34	***
	25	100 ± 8	29	—	83 ± 8	34	NS
	50	100 ± 8	18	—	94 ± 12	20	NS
(2 mM)	5	10 ± 13	7	**	ND	—	—
	25	11 ± 29	7	*	ND	—	—
	50	38 ± 42	6	NS	ND	—	—
(10 mM)	5	7 ± 5	6	***	7 ± 8	8	***, $
	25	11 ± 22	6	*	17 ± 20	8	**, $
	50	29 ± 63	4	NS	35 ± 29	6	*, NS
BAPTA							
(0.5 mM)	5	29 ± 8	21	***	13 ± 5	10	***, $
	25	52 ± 11	20	*	57 ± 17	10	NS, NS
	50	94 ± 19	12	NS	90 ± 18	8	NS, NS
(2 mM)	5	27 ± 10	10	ND	ND	—	—
	25	28 ± 17	10	*	ND	—	—
	50	34 ± 37	8	*	ND	—	—
(10 mM)	5	−7 ± 9	9	***	1 ± 8	6	***, $
	25	10 ± 19	9	**	−9 ± 23	6	**, $
	50	7 ± 40	7	**	−6 ± 34	4	**, $
APV plus MK-801	5	−5 ± 13	10	***	3 ± 7	9	***, $$
	25	7 ± 26	10	**	−3 ± 13	9	***, $$
	50	−10 ± 49	7	**	−16 ± 23	4	***, $
Unpaired	5	−7 ± 7	8	***	ND	—	—
	25	−30 ± 13	8	***	ND	—	—
	50	5 ± 13	7	***	ND	—	—
100-Hz tetanus	5	68 ± 9	14	NS	7 ± 13	8	***
	25	26 ± 22	6	*	ND	—	—
	50	21 ± 31	6	**	ND	—	—

% pot., Percent potentiation relative to wt low EGTA (0–0.5 mM) averaged over 5 min at the specific time. *n*, Number of experiments. *t* test, *P* value for two-sampled *t* test vs. wt low EGTA (NS, not significant; *, $P < .05$; **, $P < .01$; ***, $P < .0001$). *P* value for two-sampled *t* test vs. GluR-A$^{-/-}$ low EGTA (NS, not significant; $, $P < .05$; $$, $P < .01$). ND, Not determined.

EPSP amplitude in this pathway after pairing (≈14% of paired pathway at 50 min). This potentiation could represent either undetected overlap of the two pathways (see *Methods*), a consequence of whole-cell recording, or genuine heterosynaptic potentiation. For the remainder of the data presented, the changes in the control pathway are subtracted from the paired pathway as shown in the solid line in Fig. 1*B*.

Fig. 1*C* (open circles) illustrates the effect of TBP in hippocampal slices from GluR-A subunit-deficient mice. TBP results in a small initial potentiation that develops slowly with time, eventually reaching the same level as in wt (Fig. 1*C*; Table 1). Thus, TBP induces a larger than 2-fold increase in synaptic efficacy in both wt and GluR-A$^{-/-}$ mice. Fig. 1*C* (solid line) illustrates the difference in EPSP amplitudes of TBP potentiation in wt and GluR-A$^{-/-}$ mice. The initially expressed component of TBP potentiation (iniTBP) was greatly reduced in GluR-A$^{-/-}$ animals. On the other hand, the delayed component (delTBP) is very similar in both genotypes after about 25 min postpairing. This difference in the time course of potentiation suggests that associative pairing of evoked EPSPs and back-propagating APs induces at least two sorts of increases in synaptic efficacy, an early, rapidly expressed component that depends on the availability of GluR-A subunits and a delayed, slowly increasing component that is GluR-A subunit independent. Neither iniTBP nor delTBP potentiation was induced with *N*-methyl-D-aspartate (NMDA) receptor blockade or if the EPSPs and APs were unpaired, that is, presented 1 min apart (Table 1, APV plus MK-801 and Unpaired, respectively).

Although theta-burst stimulation, patterned after naturally occurring activity, has been suggested to be optimal for LTP induction (10), the majority of LTP studies have used a high frequency tetanus for induction. In our experimental conditions, a 100-Hz tetanus (1 s) induced a large initial potentiation in wt mice, similar to that found with TBP (Fig. 2*A*, open circles; Table 1). Unlike with TBP, however, this initial increase in EPSP amplitude continues to decay after induction, resulting in a level of potentiation significantly less than that obtained with TBP (Table 1, 100Hz). Subtracting the tetanus-induced potentiation from TBP potentiation (filled circles) reveals a difference component (bold line) that is nearly identical to TBP potentiation found in GluR-A$^{-/-}$ mice (light line). These results show that, in whole-cell voltage recordings from wt mice, the 100-Hz tetani, even though suprathreshold (Fig. 2*B Upper* trace), do not induce the GluR-A-independent component of TBP potentiation.

On the other hand, the potentiation induced with a 100-Hz tetanus is similar to iniTBP potentiation in time course, amplitude, and GluR-A dependence. In wt mice, TBP elicited 10 min after tetanus (Fig. 2*C*, open circles) resulted in an initial potentiation larger than with TBP alone (Fig. 2*C*, filled circles), but that decreases over time. The difference trace (solid line) resembles iniTBP potentiation and 100-Hz tetanus-induced potentiation in wt (Fig. 1*C*, solid line and Fig. 2*A*, open circles, respectively). Whereas these results show that 100-Hz tetanus does not occlude TBP potentiation, they cannot be interpreted as showing different mechanisms of induction or expression for 100-Hz tetanus and iniTBP potentiation because LTP is not saturated with a single tetanus (11). Fig. 2*D* shows in whole-cell recordings, as was previously shown in field potential recordings (7), that 100-Hz tetani fail to induce potentiation in GluR-A$^{-/-}$ mice (open circles, first 10 min). In the same cells, however, TBP elicits potentiation (open circles, 10–60 min), nearly identical to that found with TBP alone (filled circles). The absence of tetanus-induced potentiation in GluR-A$^{-/-}$ mice was not due to insufficient depolarization because the number of APs evoked by the tetanus was not significantly different from wt mice (Fig. 2*B*).

GluR-A$^{-/-}$ mice, expressing delTBP but not iniTBP potentiation, can thus be used as a tool to isolate these two forms of potentiation. We examined the relation between the magnitude of potentiation in GluR-A$^{-/-}$ mice and several cellular properties. One highly correlated factor, the presence of "complex spiking" during TBP, is displayed in Fig. 3. The bold trace in Fig. 3*A* shows a typical voltage response to the postsynaptic current injections during TBP: four of the five current injections elicit an AP. When paired with EPSPs, an additional putative Ca^{2+}-dependent AP is evoked after the current injections (dashed trace). In some cases, this additional activity took the form of a burst of APs as shown in the dashed trace in Fig. 3*B*. One third of GluR-A$^{-/-}$ and 40% of wt slices, however, showed no complex spiking with TBP (Fig. 3*B Right*, bold trace). The potentiation reached 50 min after TBP was significantly greater in those cells where complex spiking occurred, especially in GluR-A$^{-/-}$ mice (Fig. 3*C*, wt $P < 0.05$, GluR-A$^{-/-}$ $P < 0.001$). In TBP experiments where NMDA receptors were blocked, the frequency of complex spiking was greatly reduced (0/11 wt, 1/7 GluR-A$^{-/-}$, data not shown).

Whereas it is well documented that tetanus-induced LTP requires a postsynaptic Ca^{2+} influx in CA1 neurons, we wondered whether iniTBP and/or delTBP potentiation was sensitive to postsynaptically loaded Ca^{2+} buffers (5, 12, 13). The sensitivity was tested with two buffers, a rapidly equilibrating buffer, BAPTA, and a slowly equilibrating Ca^{2+} buffer, EGTA. Control experiments were performed with 0–0.5 mM EGTA in the recording pipette. Loading a high concentration of BAPTA (10 mM) into CA1-pyramidal neurons completely eliminated TBP

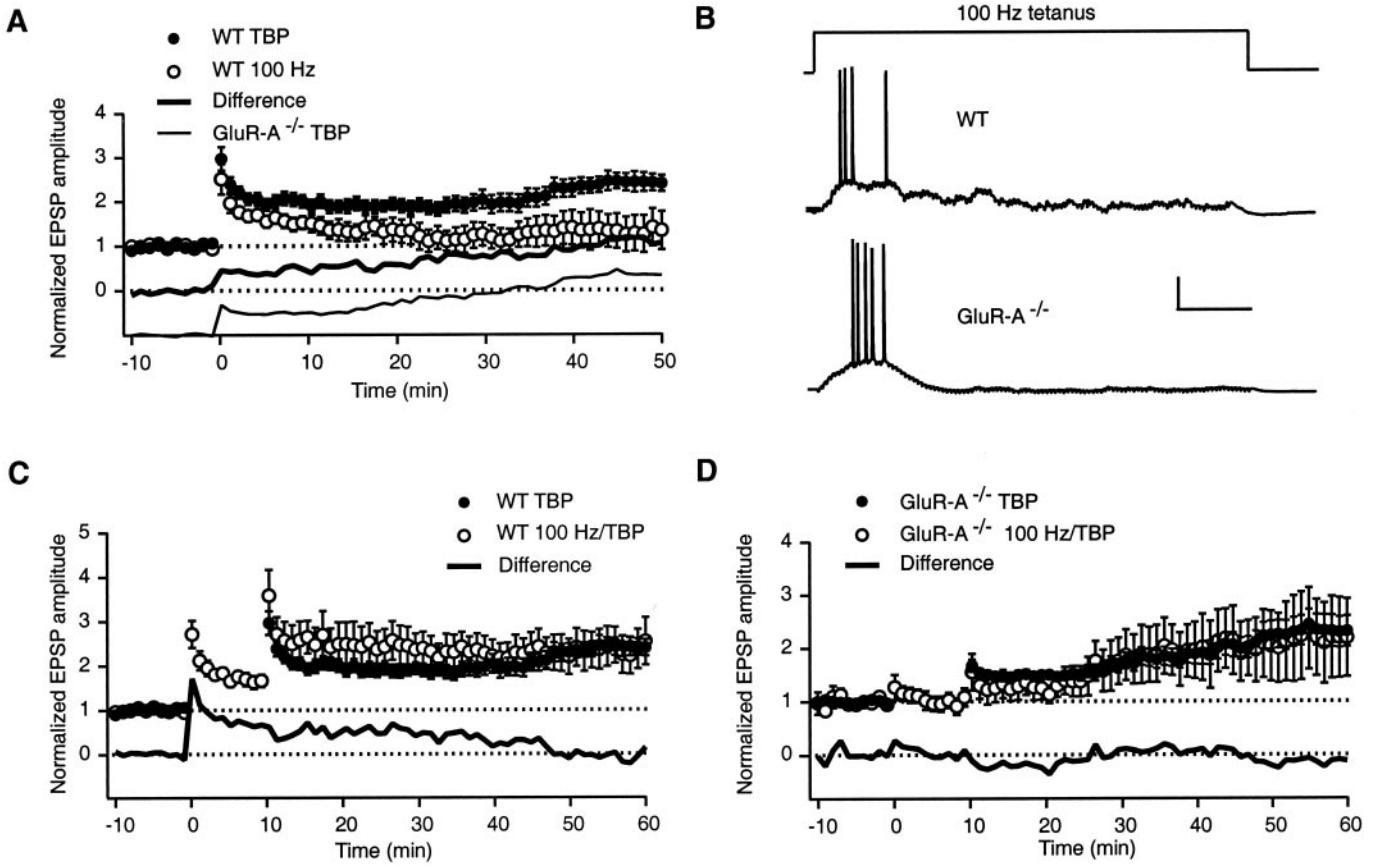

Fig. 2. The GluR-A subunit-dependent component of TBP potentiation is predominantly induced by 100-Hz tetanus. (*A*) In whole-cell recordings from *WT* mice a 1-s, 100-Hz tetanus induced a large initial potentiation (open circles) that decayed with time. A small amount of potentiation remained 50 min posttetanus. Subtracting this trace from that found with TBP in wt mice (filled circles) gives the difference component shown below (bold line). The GluR-A-dependent component of TBP potentiation (from GluR-A$^{-/-}$ mice) is shown below for comparison (light line). (*B*) Examples of voltage recordings during 100-Hz tetanus in *WT* (*Upper* trace) and GluR-A$^{-/-}$ (*Lower* trace) mice. The number of spikes recorded during 100-Hz tetanus was not significantly different between wt (16 $\pm$ 5, n = 16) and GluR-A$^{-/-}$ experiments (8 $\pm$ 6, n =8, $P > 0.3$). Scale bar = 25 mV, 200 ms. (*C*) Delivery of the 100-Hz tetanus 10 min before TBP did not occlude TBP potentiation (open circles). Subtracting this trace from TBP alone (filled circles) results in the difference trace shown below (bold line). (*D*) In GluR-A$^{-/-}$ mice, no significant potentiation was found 10 min after 100-Hz tetanus stimulation (open circles). Subsequent TBP in the same cells resulted in a potentiation nearly identical to TBP alone (filled circles). The difference trace is shown below (bold line).

potentiation in both wt (Fig. 4, Table 1) and GluR-A$^{-/-}$ mice (Table 1). Postsynaptic Ca^{2+} increase is thus required for both iniTBP and delTBP potentiation but could trigger two signal cascades. Consistent with this view, iniTBP and delTBP potentiation are differentially affected by a low concentration of BAPTA (Fig. 4, Table 1). Whereas iniTBP potentiation is greatly reduced in wt mice with 0.5 mM BAPTA (Fig. 4*A*), delTBP potentiation is not significantly affected (Fig. 4*B*) at this concentration. For iniTBP potentiation, Ca^{2+} ions entering a spine are more readily intercepted by BAPTA than by EGTA before they are able to interact with a Ca^{2+} sensor. This sensor, when occupied by Ca^{2+}, triggers a cascade of events that finally increases EPSP amplitude via a GluR-A subunit-dependent mechanism. The difference in effectiveness between EGTA and BAPTA could suggest that the site(s) of Ca^{2+} entry and the Ca^{2+} sensor for iniTBP may be separated by less than 350 nm, because EGTA is inefficient, but probably are not within molecular distance [e.g., 30 nm or closer because BAPTA is effective (14)]. For delTBP, the two buffers were equally effective. This finding could mean that a Ca^{2+} sensor for triggering delTBP is responding to a global rise in [Ca^{2+}]. It may be located further away from the entry site than the sensor for iniTBP. The BAPTA and EGTA dependence of the delTBP potentiation in GluR-A$^{-/-}$ mice is not different from wt (Table 1), suggesting that the affinity of the Ca^{2+} sensor for delTBP potentiation is unchanged in GluR-A$^{-/-}$ mice.

Discussion

The results show that a long lasting increase in synaptic efficacy can be induced by coincident suprathreshold stimulation of the pre- and postsynaptic pyramidal neurons in the hippocampus. This increase in efficacy has two components that vary inversely in their time course. The initial component, iniTBP potentiation, is maximally expressed rapidly after pairing but is decremental with time. This component depends on the GluR-A subunit and is more sensitive to internal Ca^{2+} buffers than the slowly developing, GluR-A-independent component, delTBP potentiation. Both components were found to be dependent on NMDA receptor activation.

We suggest that the two components of TBP potentiation are generated by different mechanisms. The main arguments for this view are that, in GluR-A-deficient animals, a form of potentiation persists that is identical to the delayed component of TBP-induced potentiation in wt mice 25 min after induction and that the two components display different sensitivity to postsynaptically loaded Ca^{2+} buffers. The total dendritic Ca^{2+} influx is comparable in wt and GluR-A$^{-/-}$ mice (7), suggesting that the difference between the two genotypes is located downstream of

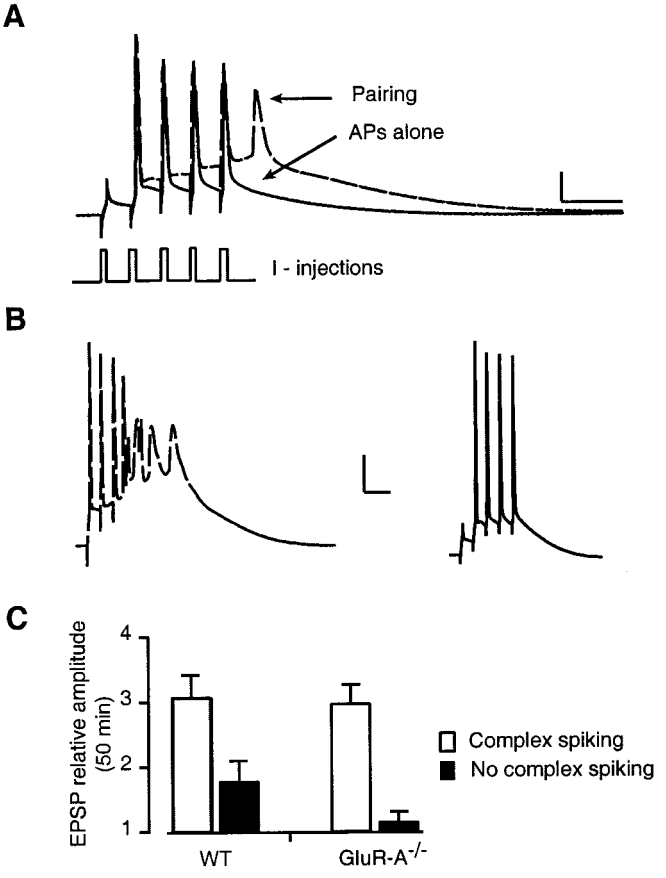

Fig. 3. Initiation of GluR-A-independent potentiation depends on complex spiking during TBP. (*A*; bold trace) Voltage recording in response to postsynaptic current injections (I-injections) used to elicit back-propagating APs. In the same cell, pairing the current injections with EPSPs resulted in an extra, putative calcium spike (dashed line). Scale bar = 20 mV, 20 ms. (*B*) TBP resulted in complex spiking in 60% (18/30) of wt and 67% (18/27) of GluR-A$^{-/-}$ experiments under normal recording conditions (*Left*, dashed trace). The remaining experiments showed no observable extra spiking in the somatic recordings (*Right*, bold trace). Scale bar = 20 mV, 20 ms. (*C*) Summary data of TBP potentiation recorded in wt and GluR-A$^{-/-}$ mice for a 5-min period ending 50 min postpairing. The data are divided into groups where complex spiking was observed during the pairing (open bars, n = 12, 9 for wt and GluR-A$^{-/-}$, respectively) and those where no complex spiking was recorded in the soma (filled bars, n = 7, 5).

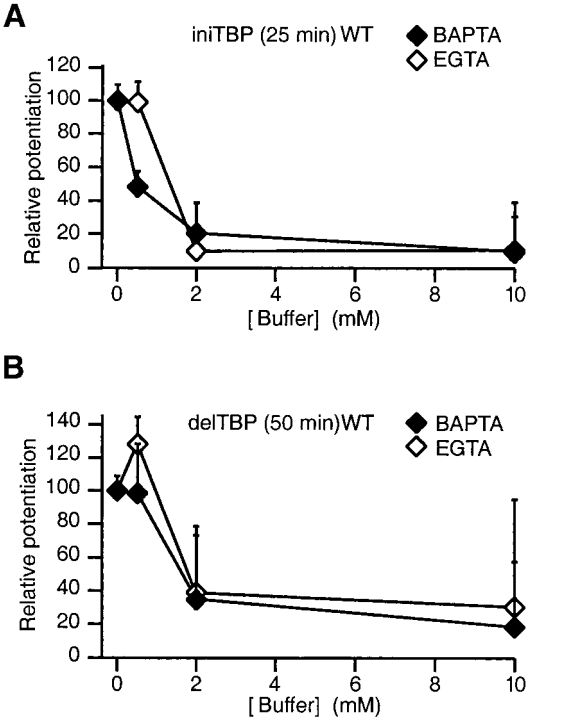

Fig. 4. Comparison of intracellularly loaded BAPTA and EGTA effectiveness in reducing ini- and delTBP potentiation in wt mice. (*A*) IniTBP potentiation measured 20–25 min after pairing. All values are relative to wt experiments with no exogenous buffers loaded. The interpolated half-effective concentration of EGTA (≈1.5 mM, open diamonds) is 3-fold higher than that for BAPTA (≈0.5 mM, filled diamonds). (*B*) DelTBP potentiation measured 45–50 min after stimulation in wt mice. The interpolated half-effective concentrations of EGTA (≈1.5 mM, open diamonds) and BAPTA (≈1.5 mM, filled diamonds) in reducing delTBP potentiation are not significantly different. The half-effective concentration of BAPTA (≈1.5 mM) for the delTBP potentiation block is higher than that for the iniTBP potentiation block (≈0.5 mM BAPTA, Fig. 4*A*).

the Ca^{2+} influx. These two mechanisms would thus diverge at the induction step where Ca^{2+} interacts with the Ca^{2+} sensor. The two cascades may operate in parallel and independently from each other. The induction may be such that one cascade (iniTBP) is preferentially activated by local Ca^{2+} influx depending on the detailed spatiotemporal [Ca^{2+}] changes in dendritic spines and shaft whereas the other cascade (delTBP) is sensitive to global [Ca^{2+}].

GluR-A-Dependent Component of TBP Potentiation. IniTBP potentiation relies on a postsynaptic mechanism of expression that depends on the availability of GluR-A subunits. This form of potentiation is also dependent on NMDAR channel activation. The iniTBP potentiation bears several similarities to tetanus-induced LTP, which has been suggested to involve either an increase in the number of postsynaptic L-α-amino-3-hydroxy-5-methylisoxazole-4-propionate receptors (AMPARs) or AMPAR conductance (3, 15–17). The results reported here are compatible with this view. Tetanus-induced LTP has frequently been suggested to be important for successful performance in the Morris water maze, a hippocampal-dependent task (18). That GluR-A$^{-/-}$ mice solve this task as well as wt mice (7, †) dissociates this form of plasticity from spatial reference memory as tested by the water maze. GluR-A$^{-/-}$ mice are, however, unable to perform above chance in the T-maze, another hippocampal-dependent task that tests spatial working memory (†, 20). The requirement for GluR-A subunits for working memory offers strong support for the assertion that the rapidly induced, transient component of TBP potentiation described here contributes to working memory as tested in the T-maze.

GluR-A-Independent Component of TBP Potentiation. The GluR-A subunit-independent component of TBP potentiation, delTBP potentiation, could (*i*) be expressed via a presynaptic mechanism, (*ii*) be expressed via a postsynaptic mechanism, or (*iii*) reflect both pre- and postsynaptic changes, possibly by an increase in the number of synaptic contacts by perforation of spines and boutons or by *de novo* spine formation (21, 22).

Activity Patterns for LTP Induction. The results support the view that naturally occurring patterns of pre- and postsynaptic activity are important for LTP induction (23). Although both 100-Hz tetani and TBP produce suprathreshold depolarization, only

†Reisel, D., Schmitt, W., Kirby, B. P., Sprengel, R., Andersen, P., Seeburg, P. H., Sakmann, B., Deacon, R. M., Bannerman, D. M. & Rawlins, J. N. (2001) *Soc. Neurosci. Abstr.*, abstr. no. 315.18.

TBP results in GluR-A-independent potentiation. Rhythmic burst firing thus appears to activate a Ca^{2+}-activated mechanism of potentiation. Such rhythmic bursting in CA1 neurons is observed when animals explore novel environments (24, 25) and has long been known to be required for spatial memory (26). One potential decoder of Ca^{2+} oscillations has been suggested to be autophosphorylation of the Ca^{2+}/calmodulin-dependent protein kinase, CaMK II (19).

This work was supported by Alexander Von Humboldt and Human Frontiers Long-Term Fellowships to D.H. and by the Volkswagen-Stiftung.

1. Malenka, R. C. & Nicoll, R. A. (1999) *Science* **285,** 1870–1874.
2. Chen, H. X., Otmakhov, N. & Lisman, J. (1999) *J. Neurophysiol.* **82,** 526–532.
3. Liao, D., Hessler, N. A. & Malinow, R. (1995) *Nature (London)* **375,** 400–404.
4. Gustafsson, B., Wigstrom, H., Abraham, W. C. & Huang, Y. Y. (1987) *J. Neurosci.* **7,** 774–780.
5. Magee, J. C. & Johnston, D. (1997) *Science* **275,** 209–213.
6. Pike, F. G., Meredith, R. M., Olding, A. W. & Paulsen, O. (1999) *J. Physiol. (London)* **518,** 571–576.
7. Zamanillo, D., Sprengel, R., Hvalby, O., Jensen, V., Burnashev, N., Rozov, A., Kaiser, K. M., Koster, H. J., Borchardt, T., Worley, P., *et al*. (1999) *Science* **284,** 1805–1811.
8. Mack, V., Burnashev, N., Kaiser, K. M., Rozov, A., Jensen, V., Hvalby, O., Seeburg, P. H., Sakmann, B. & Sprengel, R. (2001) *Science* **292,** 2501–2504.
9. Thomas, M. J., Watabe, A. M., Moody, T. D., Makhinson, M. & O'Dell, T. J. (1998) *J. Neurosci.* **18,** 7118–7126.
10. Larson, J., Wong, D. & Lynch, G. (1986) *Brain Res.* **368,** 347–350.
11. Schulz, P. E. & Fitzgibbons, J. C. (1997) *J. Neurophysiol.* **78,** 321–334.
12. Jaffe, D. B., Johnston, D., Lasser-Ross, N., Lisman, J. E., Miyakawa, H. & Ross, W. N. (1992) *Nature (London)* **357,** 244–246.
13. Spruston, N., Schiller, Y., Stuart, G. & Sakmann, B. (1995) *Science* **268,** 297–300.
14. Neher, E. (1998) *Cell Calcium* **24,** 345–357.
15. Barria, A., Muller, D., Derkach, V., Griffith, L. C. & Soderling, T. R. (1997) *Science* **276,** 2042–2045.
16. Shi, S. H., Hayashi, Y., Petralia, R. S., Zaman, S. H., Wenthold, R. J., Svoboda, K. & Malinow, R. (1999) *Science* **284,** 1811–1816.
17. Benke, T. A., Luthi, A., Isaac, J. T. & Collingridge, G. L. (1998) *Nature (London)* **393,** 793–797.
18. Martin, S. J., Grimwood, P. D. & Morris, R. G. (2000) *Annu. Rev. Neurosci.* **23,** 649–711.
19. De Konick, P. & Schulman, H. (1998) *Science* **279,** 227–230.
20. Olton, D. S. & Papas, B. C. (1979) *Neuropsychologia* **17,** 669–682.
21. Toni, N., Buchs, P. A., Nikonenko, I., Bron, C. R. & Muller, D. (1999) *Nature (London)* **402,** 421–425.
22. Engert, F. & Bonhoeffer, T. (1999) *Nature (London)* **399,** 66–70.
23. Paulsen, O. & Sejnowski, T. J. (2000) *Curr. Opin. Neurobiol.* **10,** 172–179.
24. Otto, T., Eichenbaum, H., Wiener, S. I. & Wible, C. G. (1991) *Hippocampus* **1,** 181–192.
25. O'Keefe, J. (1993) *Curr. Opin. Neurobiol.* **3,** 917–924.
26. Winson, J. (1978) *Science* **201,** 160–163.